Mechanics of Advanced Composite Structures 2 (2015) 1-16

Semnan University

Mechanics of Advanced Composite Structures

journal homepage: http://macs.journals.semnan.ac.ir

Transverse Vibration for Non-uniform Timoshenko Nano-beams

K. Torabi*, M. Rahi, H. Afshari

Department of Solid Mechanics, Faculty of Mechanical Engineering, University of Kashan, Kashan, Iran

PAPER INFO

Paper history:
Received 30 October 2014
Received in revised form 21 October 2015
Accepted 27 October 2015

Keywords:
Nonlocal elasticity
Gravity
Timoshenko
Non-uniform nano-beam
Generalized differential quadrature method

ABSTRACT

In this paper, Eringen's nonlocal elasticity and Timoshenko beam theories are implemented to analyze the bending vibration for non-uniform nano-beams. The governing equations and the boundary conditions are derived using Hamilton's principle. A Generalized Differential Quadrature Method (GDQM) is utilized for solving the governing equations of non-uniform Timoshenko nano-beam for pinned-pinned, clamped–clamped, clamped–pinned, clamped–free, clamped–slide, and pinned-slide boundary conditions. The non-dimensional natural frequencies and the normalized mode shapes are obtained for short and stubby nano-beams where influences varying cross-section area, small scale, shear deformation, rotational moment of inertia, acceleration gravity and the self-weight of the non-uniform Timoshenko nano-beam are discussed. The present study illustrates that the small scale effects are more significant for smaller size of nano-beam, larger nonlocal parameter and higher vibration modes. Further, the compression forces due to gravity and the self-weight of the nano-beam also like the small scale effect are reduced the magnitude of the frequencies of the nano-beam.

1. Introduction

The progress of nanotechnology has enthused scientists in their search of producing all sorts of micro/nanostructures such as atomic force microscope cantilever tips, nanowires, nanoactuators, nanoprobes and nano-beams. Whenever the Euler–Bernoulli beam theory and the Timoshenko beam theory are applied to the analysis of the small beam-like structures, the researchers are found to be inadequate. Being scale free, these classical beam theories could not capture the small scale effect in the mechanical properties. For example, Wang and Hu [1] showed that the classical beam theories are not able to predict the decrease in phase velocities of wave propagation in carbon nano-tubes when the wave number is so large that the nanostructure has a significant influence on the flexural wave dispersion.

In 1972, Eringen [2], Eringen and Edelen [3] and later Eringen [4,5] initiated the nonlocal continuum mechanics to allow for the small scale effect by specifying the stress state at a given point to be a function of the strain states at all points in the body. Then the nonlocal theory of elasticity has been used to study lattice dispersion of elastic waves, wave propagation in composites, dislocation mechanics, fracture mechanics, surface tension fluids, etc. [6-10] , and Wang et al. [11] used the nonlocal elasticity constitutive equations to investigate the vibration of carbon nanotubes. Wang et al. [11] neglected the nonlocal effect in writing the shear stress–strain relation of the Timoshenko beam theory (TBT), and therefore the effect of including nonlocal constitutive behavior amounted to using an equivalent shear correction factor.

Reddy [12] used various available beam theories, including the Timoshenko beam theory, are reformulated using the nonlocal differential constitutive

* Corresponding author. Tel: +98-361-5912448, Fax +98-361-5559930

E-mail address: kvntrb@kashanu.ac.ir

relations of Eringen. Wang et al. [13] analyzed the vibration of nonlocal Timoshenko beams.

This paper presents a formulation of nonlocal elasticity theory for the transverse vibration analysis of non-uniform Timoshenko nano-beams (NUTNB). The differential equations of motion are employed to derive from the variational procedure (Hamilton's principle) and the solutions numerically calculated using GDQM for pinned-pinned, clamped-clamped, clamped-pinned, clamped-free, clamped-slide and pinned-slide boundary conditions. This study makes the first attempt to study the axially distributed forces such as an integration-form varying compression force due to gravity acceleration on NUTNB. In addition the small scale effects, Timoshenko parameters and axial loading are investigated for non-uniform (tapered) nano-beam. The main purpose of this article is to investigate the vibrational response of NUTNB with axial loading for arbitrary boundary conditions and for various values of the small scale effects. This study is organized as follows. Firstly, in Section 2, the nonlocal elasticity theory of Eringen is presented using the nonlocal constitutive differential equations. Secondly, in Section 3, the governing differential equations describing the transverse vibrations will be derived for NUTNB. Also, the present paper is concerned with the gravity effect on the vibration behavior of nano-beams. Then, in Section 4, the solution procedure and dimensionless equations will be derived from some of the various boundary conditions. In Section 5 the numerical solution of the problem will be solved approximately using GDQM and the matrix form will be transformed for equations of motion. Also in Section 6, the numerical results obtained from the present analysis are discussed in many cases of nano-beam. Finally, in Section 7 conclusions will be drawn and remarks the results of presenting work.

2. Nonlocal Elasticity Theory of Eringen

The classical elasticity theory presents the constitutive equation in the form of an algebraic relationship between the stress and strain tensors while that of the nonlocal elasticity theory according to Eringen [2-5], is that the stress field at a reference point x in an elastic continuum depends not only on the strain at that point but likewise on the strains at all other points in the body. Eringen's nonlocal elasticity involves spatial integrals which represents weighted averages of the contributions of strain tensors of all points in the body to the stress tensor at the given point. Eringen attributed this fact to the atomic theory of lattice dynamics and experimental observations on phonon dispersion [12]. The scale effects are accounted for in the theory by considering the internal size as a material parameter [14].

2.1. The Constitutive Relations

The basic equations for linear, homogeneous, isotropic, nonlocal elastic solid with zero body force are given by [15],

$$\sigma = \int_V K\left(|x'-x|,\tau\right)t\left(x'\right)dx' \tag{1}$$

where σ is the nonlocal stress tensor, $t(x')$ is the classical, the macroscopic stress tensor at point x and the kernel function $K(|x'-x|, \tau)$ are the nonlocal moduli, or attenuation function incorporating into constitutive equations the nonlocal effects at the reference point x are produced by local strain at the source x', τ is the material constant which is defined as $\tau=e_0a/l$ where e_0 is a constant appropriate to each material, a is an internal characteristics length (e.g., lattice parameter, granular distance) and l is an external characteristics length (e.g., crack length, wavelength).

The constitutive Eq. (1) defines the nonlocal constitutive behavior of a Hookean solid and represents the weighted average of the contributions of the strain field of all points in the body to the stress field at a point. Though the integral constitutive relation in Eq. (1) makes mathematical difficulties to obtain the solution of nonlocal elasticity problems, Eringen [4] represents this integral constitutive equation to equivalent differential constitutive equations under certain conditions. For an elastic material in the one dimensional case, the nonlocal constitutive relations may be simplified as [4,13].

2.2. Stress Resultant

The nonlocal constitutive can be approximated to a one-dimensional form, in terms of the strains in the Timoshenko beam theory (TBT) [16],

$$\sigma_{xx} - \mu\frac{\partial^2\sigma_{xx}}{\partial x^2} = E\varepsilon_{xx} \tag{2}$$

$$\sigma_{xz} - \mu\frac{\partial^2\sigma_{xz}}{\partial x^2} = G\gamma_{xz} \tag{3}$$

where E and G are the Young's and shear moduli, respectively, and γ is the shear strain. Hence, the nonlocal parameter $\mu=(e_0a)^2$, a in the theory will be led to small-scale effect on the response of structures of nano-size and when μ is zero, the constitutive relations will be derived of the local theories.

3. Nonlocal Equations of NUTNB

3.1. The Governing Equations of Motion

The Timoshenko beam theory (TBT), which is based on the displacement field at some points, can be found in [17,18].

All applied loads and geometry are such that the displacements (u_1,u_2,u_3) along the coordinates (x,y,z) are only functions of the x and z coordinates and time t. The displacement u_2 is supposed identically zero. The terms u and w are the axial and transverse displacements, respectively, of the point (x,0) on the mid-plane (i.e., z = 0) of the beam and the ϕ denotes the rotation of the cross-section. The nonzero strains according to TBT are expressed as,

$$\varepsilon_{xx} = \frac{\partial u_1(x,z,t)}{\partial x} = \frac{\partial u(x,t)}{\partial x} + z\frac{\partial \varphi(x,t)}{\partial x}$$
$$\gamma_{xz} = 2\varepsilon_{xz} = \frac{\partial u_1(x,z,t)}{\partial z} + \frac{\partial u_3(x,z,t)}{\partial x}$$
$$\gamma_{xz} = \varphi(x,t) + \frac{\partial w(x,t)}{\partial x} \tag{4}$$

The nonlocal bending moment M, and the shear force Q, can be written in the following form,

$$M(x,t) = \int_A \sigma_{xx} z dA \tag{5}$$

$$Q(x,t) = \int_A \sigma_{xz} dA. \tag{6}$$

where σ_{xx} is the normal stress and σ_{xz} the transverse shear stress. A is the cross-sectional area of the beam. The following relations are introduced for using in the coming sections,

$$A = \int_A dA \ , \quad \int_A z\, dA = 0 \ , \quad I = \int_A z^2 dA \tag{7}$$

Therefore, the x-axis is taken along the geometric centric of the beam, where I is the second moment of area of the cross-section.

In this stage, by multiplying both sides of Eq. (2) by z and integrating over the cross-section area of the beam, then using Eqs. (4) to (7) , the nonlocal Timoshenko constitutive relations yields,

$$M(x,t) - \mu\frac{\partial^2 M(x,t)}{\partial x^2} = EI(x)\frac{\partial \phi(x,t)}{\partial x} \tag{8}$$

Also, by integrating Eq. (3) over the area, and using Eqs. (4) to (7), one obtains,

$$Q(x,t) - \mu\frac{\partial^2 Q(x,t)}{\partial x^2} = GK_s A(x)\left[\frac{\partial w(x,t)}{\partial x} + \phi(x,t)\right] \tag{9}$$

where K_s denotes the shear correction factor of TBT in order to compensate for the error in assuming a constant shear strain (stress) through the thickness of the beam. The shear correction factors depend not only on the material and geometric parameters but also on the load and boundary conditions.

The shear correction factor is 9/10 for a circular shape cross-section and 5/6 for a rectangular cross-section [11]. A value of 0.877 was used by Reddy and Pang [19] for the analysis of carbon nanotubes (CNTs) with the relation $K_s = (5+5\nu)/(6+5\nu)$ for the rectangle and $K_s = (6+12\nu+6\nu^2)/(7+12\nu+4\nu^2)$ for the circle in which ν is Poisson's ratio with value of ν = 0.3 [20]. The strain energy U and the kinetic energy T of the beam are obtained, respectively, by the following equations [21],

$$T(t) = \frac{1}{2}\int_0^L \rho A(x)\left[\left(\frac{\partial u_1}{\partial t}\right)^2 + \left(\frac{\partial u_3}{\partial t}\right)^2\right]dx,$$
$$U(t) = \frac{1}{2}\int_0^L \int_A (\sigma_{xx}\varepsilon_{xx} + \sigma_{xz}\gamma_{xz})dA\,dx \tag{10}$$

where ρ is the mass density of the nano-beam material.

By substituting Eqs. (4) to (7), into the above energy statements, and neglecting axial displacement of the neural web $u(x,t)$, the kinetic and strain energies with respect to the displacement field may be expressed as,

$$T(t) = \frac{1}{2}\int_0^L \left\{\rho I(x)\left[\frac{\partial \varphi(x,t)}{\partial t}\right]^2 + \rho A(x)\left[\frac{\partial w(x,t)}{\partial t}\right]^2\right\}dx$$
$$U(t) = \frac{1}{2}\int_0^L \left\{\begin{matrix} M(x,t)\dfrac{\partial \varphi(x,t)}{\partial x} + \\ Q(x,t)\left[\dfrac{\partial w(x,t)}{\partial x} + \varphi(x,t)\right]\end{matrix}\right\}dx \tag{11}$$

In addition, the work done by the external axial force is denoted by,

$$W(t) = -\frac{1}{2}\int_0^L P(x)\left[\frac{\partial w(x,t)}{\partial x}\right]^2 dx \tag{12}$$

where P is the distributed axial load along x axis. The Hamilton's principle is the most powerful variational principle of mechanics, hence the principle of virtual displacements for the TBT is given by,

$$\delta\int_{t_0}^{t_1}\left[T(t) - U(t) + W(t)\right]dt = 0 \tag{13}$$

Therefore, by substituting Eqs. (11) and (12) into Eq. (13),then, integrating by parts and since δw and $\delta\phi$ are arbitrary in the domain of nano-beam and then setting the coefficients of δw and $\delta\phi$ to zero lead to the Euler–Lagrange equations of motion in $0 < x < L$ as [22],

$$\frac{\partial M(x,t)}{\partial x}-Q(x,t)=\rho I(x)\frac{\partial^2\varphi(x,t)}{\partial t^2}$$
$$\frac{\partial Q(x,t)}{\partial x}+\frac{\partial}{\partial x}\left[P(x)\frac{\partial w(x,t)}{\partial x}\right]=$$
$$\rho A(x)\frac{\partial^2 w(x,t)}{\partial t^2} \quad (14)$$

The corresponding boundary conditions involve specifying one element of each of the following three pairs at the end of $x = 0$ and $x = L$,

$$\varphi(x,t)=0 \quad or \quad M(x,t)=0$$
$$w(x,t)=0 \quad or$$
$$V(x,t)=Q(x,t)+P(x)\frac{\partial w(x,t)}{\partial x} \quad (15)$$

where V denotes the equivalent shear force. By substituting Eq. (14) into the implicit Eqs. (8) and (9), the explicit expressions of the nonlocal bending moment M and shear force Q can be obtained as,

$$M(x,t)=EI(x)\frac{\partial\varphi(x,t)}{\partial x}-$$
$$\mu\left(\frac{\partial}{\partial x}\left[P(x)\frac{\partial w(x,t)}{\partial x}\right]-\right.$$
$$\left.\frac{\partial^2}{\partial t^2}\left\{\frac{\partial}{\partial x}\left[\rho I(x)\varphi(x,t)\right]+\rho A(x)\,w(x,t)\right\}\right)$$
$$Q(x,t)=G\,K_s A(x)\left[\varphi(x,t)+\frac{\partial w(x,t)}{\partial x}\right]-$$
$$\mu\frac{\partial}{\partial x}\left\{\frac{\partial}{\partial x}\left[P(x)\frac{\partial w(x,t)}{\partial x}\right]-\rho A(x)\frac{\partial^2 w(x,t)}{\partial t^2}\right\} \quad (16)$$

Then, the Euler–Lagrange equations of motion for the nonlocal NUTNB can be derived by inserting Eq. (16) into Eq. (14),

$$\frac{\partial}{\partial x}\left[E\,I(x)\frac{\partial\varphi(x,t)}{\partial x}\right]-G\,K_s A(x)\left[\varphi(x,t)+\frac{\partial w(x,t)}{\partial x}\right]=$$
$$\frac{\partial^2}{\partial t^2}\left\{\rho I(x)\varphi(x,t)-\mu\frac{\partial^2}{\partial x^2}\left[\rho A(x)w(x,t)\right]\right\},$$
$$\frac{\partial}{\partial x}\left\{G\,K_s A(x)\left[\varphi(x,t)+\frac{\partial w(x,t)}{\partial x}\right]\right\}-$$
$$\mu\frac{\partial^3}{\partial x^3}\left[P(x)\frac{\partial w(x,t)}{\partial x}\right]+\frac{\partial}{\partial x}\left[P(x)\frac{\partial w(x,t)}{\partial x}\right]=$$
$$\frac{\partial^2}{\partial t^2}\left\{\rho A(x)w(x,t)-\mu\frac{\partial^2}{\partial x^2}\left[\rho A(x)w(x,t)\right]\right\} \quad (17)$$

3.2. The Gravity Acceleration

One kind of the axial force is the influence of gravity. Now in the present study, the transverse vibration characteristics of NUTNB will be analyzed in two cases, with or without axial force. In case with axial force, there are also two cases, one is a NUTNB subjected to the constant axial force and the other is of a cantilever NUTNB under axially distributed gravity force.

Due to the gravity and the self-weight of the nano-beam an integration-form varying compression or tensile force is acting on the nano-beam. The force of non-uniform cantilever nano-beam (Clamped-Free) due to acceleration gravity given by,

$$P_S(x)=-\rho g\int_x^L A(x)dx \quad (18)$$

$$P_H(x)=+\rho g\int_x^L A(x)dx \quad (19)$$

where compressive force P_S is used for a standing beam and tensile force P_H is used for a hanging one.

4. The Solution Procedure and Dimensionless Equations

A general solution is assumed in the form,

$$w(x,t)=W(x)e^{i\omega t},\quad \varphi(x,t)=\Phi(x)e^{i\omega t} \quad (20)$$

where W and Φ are the amplitude of the generalized displacements and rotation of beam, respectively, ω the vibration frequency of NUTNB and i^2=-1. For convenience and simplification, the governing equations can be expressed in the non-dimensional form by introducing the following dimensionless parameters [13,14,23],

$$\bar{x}=\frac{x}{L},\qquad \bar{w}=\frac{W(x)}{L},\qquad \bar{A}(\bar{x})=\frac{A(x)}{A_0},$$
$$\bar{I}(\bar{x})=\frac{I(x)}{I_0},\qquad \bar{P}(\bar{x})=\frac{P(x)}{P_0},\qquad \lambda^2=\frac{\rho A_0 L^4\omega^2}{EI_0},$$
$$\xi^2=\frac{A_0L^2}{I_0},\qquad \Omega=\frac{EI_0}{G\,K_s A_0 L^2},\qquad \alpha^2=\frac{\mu}{L^2},$$
$$\varepsilon=\frac{\rho g A_0 L^3}{EI_0},\qquad \bar{p}=\frac{P_0}{G\,K_s A_0},\qquad \bar{M}=\frac{ML}{EI_0},$$
$$\bar{V}=\frac{V}{G\,K_s A_0},\qquad \bar{p}_g=\varepsilon\Omega,\qquad \bar{P}_g(\bar{x})=\int_{\bar{x}}^1\bar{A}(\bar{x})d\bar{x}. \quad (21)$$

where λ is the non-dimensional natural frequency, ζ is the slenderness ratio, α is the scaling effect parameter of the nano-beam, Ω is the shear deformation parameter, $\bar{M}$ is the non-dimensional bending moment, $\bar{p}$ and V are the non-dimensional axial and shear forces, respectively, ε is the gravity parameter, $\bar{p}_g$and $\bar{P}_g$ are the non-dimensional coefficient and function of the axial force due to gravity, respectively. It should be noted that in the case with gravity, the following statements are used,

$$\bar{p} = \bar{p}_g,\ \ \bar{P}(\bar{x}) = \bar{P}_g(\bar{x}) \tag{22}$$

By substituting Eqs. (20) and (21), into governing equations and corresponding boundary conditions, the nonlocal governing equations for NUTNB in dimensionless form yields,

$$\frac{\lambda^2\Omega}{\xi^2}\left[\bar{I}\,\bar{\varphi} - \alpha^2\frac{d^2}{d\bar{x}^2}\left(\bar{I}\,\bar{\varphi}\right)\right] + \Omega\frac{d}{d\bar{x}}\left(\bar{I}\frac{d\bar{\varphi}}{d\bar{x}}\right) - \bar{A}\left(\frac{d\bar{w}}{d\bar{x}} + \bar{\varphi}\right) = 0$$

$$\frac{d}{d\bar{x}}\left[\bar{A}\left(\frac{d\bar{w}}{d\bar{x}} + \bar{\varphi}\right)\right] + \lambda^2\Omega\left[\bar{A}\bar{w} - \alpha^2\frac{d^2}{d\bar{x}^2}\left(\bar{A}\bar{w}\right)\right] - \bar{p}\left[\alpha^2\frac{d^3}{d\bar{x}^3}\left(\bar{P}\frac{d\bar{w}}{d\bar{x}}\right) - \frac{d}{d\bar{x}}\left(\bar{P}\frac{d\bar{w}}{d\bar{x}}\right)\right] = 0 \tag{23}$$

The natural boundary conditions are as,

$$\bar{M} = \bar{I}\frac{d\bar{\varphi}}{d\bar{x}} - \alpha^2\left\{\begin{array}{l}\lambda^2\left[\frac{1}{\xi^2}\frac{d}{d\bar{x}}\left(\bar{I}\,\bar{\varphi}\right) + \left(\bar{A}\bar{w}\right)\right] \\ + \frac{\bar{p}}{\Omega}\frac{d}{d\bar{x}}\left(\bar{P}\frac{d\bar{w}}{d\bar{x}}\right)\end{array}\right\}$$

$$\bar{V} = \bar{A}\left(\frac{d\bar{w}}{d\bar{x}} + \bar{\varphi}\right) - \lambda^2\alpha^2\Omega\frac{d}{d\bar{x}}\left(\bar{A}\bar{w}\right) - \bar{p}\left[\alpha^2\frac{d^2}{d\bar{x}^2}\left(\bar{P}\frac{d\bar{w}}{d\bar{x}}\right) - \bar{P}\frac{d\bar{w}}{d\bar{x}}\right] \tag{24}$$

The geometry boundary conditions are as,

$$\bar{w}(\bar{x}) = 0, \quad \bar{\varphi}(\bar{x}) = 0 \tag{25}$$

Note that the nonlocal governing equations given in Eqs. (23) to (25), reduce to that of the counterpart local Timoshenko model when the nonlocal parameter or small scale effect is set to zero ($\alpha = 0$). Finally, the corresponding dimensionless boundary conditions with nano-beam are listed in Table 1.

5. Generalized Differential Quadrature Method (GDQM)

Gauss quadrature is a numerical integration method. Its basic idea is to approximate a definite integral with a weighted sum of integrand values of a group of nodes in the form of,

$$\int_a^b f(x)dx \approx \sum_{j=1}^{N} w_j f(x_j) \tag{26}$$

where x_j are nodes and w_j are weighting coefficients.

In the differential quadrature method (DQM) the weighting coefficients are determined by solving a system of linear equations. Extending Gauss quadrature to find the derivatives of various orders of a differentiable function gives a rise to the differential quadrature [24,25].

In other words, the derivatives of a function are approximated by weighted sums of the function values in a group of nodes [26,27].

The two major disadvantages of DQM are: the first limits, the small number of grid points and requires solving sets of linear equations, the second limits the distribution of the grid points which is critical in structural dynamic analysis. In GDQM the weighting coefficients for derivative approximations are given by a simple algebraic expression and a recurrence relationship, together with arbitrary choices of grid points [27-30]. Consider the discretization of mth order derivative of $w(x)$, the following DQ approximation is assumed as,

$$\frac{\partial^m w(x_i,t)}{\partial x^m} = \sum_{j=1}^{N} C_{ij}^{(m)}\, w(x_j,t) \tag{27}$$

where C_{mij} are weighting coefficients for mth derivative and $w(x_j)$ are function values at grid points x_j (i = 1,2,...,N). Therefore, explicit formulas for these coefficients are found to be [26,29],

$$C_{ij}^{(1)} = \frac{M^{(1)}(x_i)}{(x_i - x_j)M^{(1)}(x_j)}$$

$$C_{ij}^{(m)} = m\left(C_{ii}^{(m-1)} - \frac{C_{ij}^{(m-1)}}{x_j - x_i}\right),$$

$$i, j = 1,2,...,N, i \neq j, m = 2,3,...,N-1$$

$$C_{ii}^{(m)} = -\sum_{\substack{j=1 \\ j\neq i}}^{N} C_{ij}^{(m)}, i = 1,2,...,N, m = 1,2,...,N-1 \tag{28}$$

By choosing the Lagrange interpolated polynomial $M(x)$ as the set of test functions, yields,

$$M(x) = \prod_{j=1}^{N}(x - x_j), \quad M^{(1)}(x_i) = \prod_{\substack{j=1 \\ j\neq i}}^{N}(x_i - x_j) \tag{29}$$

Higher order coefficient matrices at each grid point can be obtained in GDQM from the first order weighting matrix as follows, [31, 32],

$$\frac{d\bar{w}(\bar{x}_i)}{d\bar{x}} = \sum_{j=1}^{N} C_{ij}^{(1)}\bar{w}(\bar{x}_j)$$

$$\frac{d^2\bar{w}(\bar{x}_i)}{d\bar{x}^2} = \sum_{j=1}^{N} C_{ij}^{(2)}\bar{w}(\bar{x}_j), \quad \sum_{j=1}^{N} C_{ij}^{(2)} = \sum_{k=1}^{N} C_{ik}^{(1)}C_{kj}^{(1)}$$

$$\frac{d^3\bar{w}(\bar{x}_i)}{d\bar{x}^3} = \sum_{j=1}^{N} C_{ij}^{(3)}\bar{w}(\bar{x}_j), \quad \sum_{j=1}^{N} C_{ij}^{(3)} = \sum_{k=1}^{N} C_{ik}^{(1)}C_{kj}^{(2)}$$

$$\frac{d^4\bar{w}(\bar{x}_i)}{d\bar{x}^4} = \sum_{j=1}^{N} C_{ij}^{(4)}\bar{w}(\bar{x}_j), \quad \sum_{j=1}^{N} C_{ij}^{(4)} = \sum_{k=1}^{N} C_{ik}^{(1)}C_{kj}^{(3)} \tag{30}$$

To choose the distribution of the grid points, among non-uniform spacing of nodes which ensure the convergence, the Chebyshev nodes defined by the following equation are nearly optimal [26, 27].

Table 1. The dimensionless boundary conditions of NUTNB

Type	Boundary conditions (BCs)			
	Geometry		Natural	
Pinned (P)	$\bar{w}=0$	-	$\bar{M}=0$	-
Clamped (C)	$\bar{w}=0$	$\bar{\varphi}=0$	-	-
Free (F)	-	-	$\bar{M}=0$	$\bar{V}=0$
Slide (S)	$\bar{\varphi}=0$	-	$\bar{V}=0$	-

$$x_i = x_1 + \frac{x_N - x_1}{2}\left[1-\cos\left(\frac{i-1}{N-1}\pi\right)\right], \quad i=1,2,...,N \tag{31}$$

By the expansion of Eqs. (23) and (24), and then rewriting the resultant equations by generalizing differential quadrature (GDQ) model, the governing equations were obtained for the nonlocal NUTNB.

$$\begin{aligned}
&-\bar{A}(\bar{x}_i)\sum_{j=1}^{N}C_{ij}^{(1)}\bar{w}_j - \bar{A}(\bar{x}_i)\bar{\varphi}_i + \\
&\Omega\left[\frac{d\bar{I}(\bar{x}_i)}{d\bar{x}}\sum_{j=1}^{N}C_{ij}^{(1)}\bar{\varphi}_j + \bar{I}(\bar{x}_i)\sum_{j=1}^{N}C_{ij}^{(2)}\bar{\varphi}_j\right] + \\
&\frac{\lambda^2\Omega}{\xi^2}\left\{\begin{array}{l}\bar{I}(\bar{x}_i)\bar{\varphi}_i - \\ \alpha^2\left[\begin{array}{l}\dfrac{d^2\bar{I}(\bar{x}_i)}{d\bar{x}^2}\bar{\varphi}_i + 2\dfrac{d\bar{I}(\bar{x}_i)}{d\bar{x}}\sum_{j=1}^{N}C_{ij}^{(1)}\bar{\varphi}_j + \\ \bar{I}(\bar{x}_i)\sum_{j=1}^{N}C_{ij}^{(2)}\bar{\varphi}_j\end{array}\right]\end{array}\right\} = 0 \\
&\bar{A}(\bar{x}_i)\sum_{j=1}^{N}C_{ij}^{(2)}\bar{w}_j + \frac{d\bar{A}(\bar{x}_i)}{d\bar{x}}\sum_{j=1}^{N}C_{ij}^{(1)}\bar{w}_j - \\
&\bar{p}\left\{\begin{array}{l}\alpha^2\left[\begin{array}{l}\bar{P}(\bar{x}_i)\sum_{j=1}^{N}C_{ij}^{(4)}\bar{w}_j + 3\dfrac{d\bar{P}(\bar{x}_i)}{d\bar{x}}\sum_{j=1}^{N}C_{ij}^{(3)}\bar{w}_j \\ +3\dfrac{d^2\bar{P}(\bar{x}_i)}{d\bar{x}^2}\sum_{j=1}^{N}C_{ij}^{(2)}\bar{w}_j + \dfrac{d^3\bar{P}(\bar{x}_i)}{d\bar{x}^3}\sum_{j=1}^{N}C_{ij}^{(1)}\bar{w}_j\end{array}\right] - \\ \dfrac{d\bar{P}(\bar{x}_i)}{d\bar{x}}\sum_{j=1}^{N}C_{ij}^{(1)}\bar{w}_j - \bar{P}(\bar{x}_i)\sum_{j=1}^{N}C_{ij}^{(2)}\bar{w}_j\end{array}\right\} \\
&+\bar{A}(\bar{x}_i)\sum_{j=1}^{N}C_{ij}^{(1)}\bar{\varphi}_j + \frac{d\bar{A}(\bar{x}_i)}{d\bar{x}}\bar{\varphi}_j + \\
&\lambda^2\Omega\left\{\bar{A}(\bar{x}_i)\bar{w}_i - \alpha^2\left[\begin{array}{l}\dfrac{d^2\bar{A}(\bar{x}_i)}{d\bar{x}^2}\bar{w}_i \\ +2\dfrac{d\bar{A}(\bar{x}_i)}{d\bar{x}}\sum_{j=1}^{N}C_{ij}^{(1)}\bar{w}_j \\ +\bar{A}(\bar{x}_i)\sum_{j=1}^{N}C_{ij}^{(2)}\bar{w}_j\end{array}\right]\right\} = 0
\end{aligned} \tag{32}$$

Natural boundary conditions may be rewritten in the following statements in the form of GDQM,

$$\begin{aligned}
&\bar{M} = \frac{-\alpha^2\bar{p}}{\Omega}\left[\begin{array}{l}\dfrac{d\bar{P}(\bar{x}_i)}{d\bar{x}}\sum_{j=1}^{N}C_{ij}^{(1)}\bar{w}_j + \\ \bar{P}(\bar{x}_i)\sum_{j=1}^{N}C_{ij}^{(2)}\bar{w}_j\end{array}\right] \\
&+\bar{I}(\bar{x}_i)\sum_{j=1}^{N}C_{ij}^{(1)}\bar{\varphi}_j - \\
&\lambda^2\alpha^2\left[\begin{array}{l}\bar{A}(\bar{x}_i)\bar{w}_i + \dfrac{1}{\xi^2}\dfrac{d\bar{I}(\bar{x}_i)}{d\bar{x}}\bar{\varphi}_i + \\ \bar{I}(\bar{x}_i)\sum_{j=1}^{N}C_{ij}^{(1)}\bar{\varphi}_j\end{array}\right] \\
&\bar{V} = \bar{A}(\bar{x}_i)\sum_{j=1}^{N}C_{ij}^{(1)}\bar{w}_j - \\
&\bar{p}\left\{\alpha^2\left[\begin{array}{l}\dfrac{d^2\bar{P}(\bar{x}_i)}{d\bar{x}^2}\sum_{j=1}^{N}C_{ij}^{(1)}\bar{w}_j + \\ 2\dfrac{d\bar{P}(\bar{x}_i)}{d\bar{x}}\sum_{j=1}^{N}C_{ij}^{(2)}\bar{w}_j + \\ \bar{P}(\bar{x}_i)\sum_{j=1}^{N}C_{ij}^{(3)}\bar{w}_j\end{array}\right] - \bar{P}(\bar{x}_i)\sum_{j=1}^{N}C_{ij}^{(1)}\bar{w}_j\right\} + \\
&\bar{A}(\bar{x}_i)\bar{\varphi}_i - \lambda^2\alpha^2\Omega\left[\frac{d\bar{I}(\bar{x}_i)}{d\bar{x}}\bar{w}_i + \bar{A}(\bar{x}_i)\sum_{j=1}^{N}C_{ij}^{(1)}\bar{w}_j\right]
\end{aligned} \tag{33}$$

where the displacement vector and the rotation vector are expressed as,

$$\bar{w}_i = \left[\bar{w}_1 \;\; \bar{w}_2 \;\; ... \;\; \bar{w}_N\right]^T, \qquad \bar{\varphi}_i = \left[\bar{\varphi}_1 \;\; \bar{\varphi}_2 \;\; ... \;\; \bar{\varphi}_N\right]^T \tag{34}$$

Eqs. (32) to (34) can be easily transformed into an eigenvalue problem to obtain the non-dimensional natural frequency. For NUTNB model,

$$\begin{bmatrix}K_{11} & K_{12}\\ K_{21} & K_{22}\end{bmatrix}\begin{Bmatrix}\bar{w}\\ \bar{\varphi}\end{Bmatrix} - \lambda^2\begin{bmatrix}M_{11} & M_{12}\\ M_{21} & M_{22}\end{bmatrix}\begin{Bmatrix}\bar{w}\\ \bar{\varphi}\end{Bmatrix} = \begin{Bmatrix}0\\ 0\end{Bmatrix} \tag{35}$$

In simple form, yields

$$[K]\{\bar{z}\} - \lambda^2[M]\{\bar{z}\} = \{0\}, \quad \{\bar{z}\} \square \{\bar{w},\bar{\varphi}\}^T \tag{36}$$

And *K*, *M* are the stiffness and mass matrices, respectively. Also the nonlocal boundary conditions are expressed as,

$$\begin{aligned}
\bar{M} &= [Q]\{\bar{z}\} - \lambda^2[R]\{\bar{z}\} \\
\bar{V} &= [S]\{\bar{z}\} - \lambda^2[T]\{\bar{z}\}
\end{aligned} \tag{37}$$

The present problem has been solved for some of the Boundary Conditions (BCs.) as: Pinned-Pinned (PP), Clamped-Clamped (CC), Clamped-Pinned (CP), Clamped-Free (CF), Clamped-Slide (CS) and Pinned-Slide (PS). The BCs. have been implemented simply using GDQM technique in the following matrix form. To illustrate the technique, Consider the NUTNB pinned at the two ends,

$$\bar{w}=0,\ \bar{M}=0,\ at\ \ \bar{x}=0,1. \tag{38}$$

Eq. (37) is converted to the following form for imposition the natural BCs.

$$\begin{aligned}&\bar{M}_0=\left[Q_0\right]\{\bar{z}\}-\lambda^2\left[R_0\right]\{\bar{z}\}=0,\ \ at\,\bar{x}=0\\&\bar{M}_1=\left[Q_1\right]\{\bar{z}\}-\lambda^2\left[R_1\right]\{\bar{z}\}=0,\,at\,\bar{x}=1\end{aligned} \tag{39}$$

Therefore, Eq. (36) is transformed to,

$$\left[K_t\right]\{\bar{z}\}-\lambda^2\left[M_t\right]\{\bar{z}\}=\{0\} \tag{40}$$

$$\left[K_t\right]=\begin{bmatrix}K\\Q_0\\Q_1\end{bmatrix},\quad \left[M_t\right]=\begin{bmatrix}M\\R_0\\R_1\end{bmatrix} \tag{41}$$

Finally, for imposition the geometry BCs., one obtains,

$$\left[\bar{K}_t\right]\{\bar{z}_t\}-\lambda^2\left[\bar{M}_t\right]\{\bar{z}_t\}=\{0\} \tag{42}$$

$$\bar{z}_t=\left[\bar{w}_2\ \ldots\ \bar{w}_{N-1}\ \ \bar{\varphi}_1\ \ \bar{\varphi}_2\ \ldots\ \bar{\varphi}_N\right]^T \tag{43}$$

where the matrices in Eq. (42) have been extracted by omitting the first and *N*th the row and column, respectively. Hence, using this technique Eq. (42) can easily be reduced to an eigenvalue problem as,

$$\left[\bar{Z}_t\right]\{\bar{z}_t\}=\lambda^2\{\bar{z}_t\} \tag{44}$$

$$\left[\bar{Z}_t\right]=\left[\bar{M}_t\right]^{-1}\left[\bar{K}_t\right] \tag{45}$$

Eq. (44) can be solved by a standard eigenvalue solver, and then the non-dimensional nonlocal natural frequencies of the NUTNB are obtained.

6. Numerical Results and Discussions

6.1. The Technique Verification

Firstly, the bending vibration of a uniform clamped–free Timoshenko beam with the rotary inertia parameter r^2 = 0.01 and 0.001; and the shear deformation parameter s^2 = 2.8 and 0.5 [23] is considered by following statements,

$$\xi^2=\frac{1}{r^2},\quad \Omega=r^2.s^2 \tag{46}$$

The first ten non-dimensional natural frequencies are shown in Table 2. The result in this Table, yields highly agreement with the result of the exact solution of Hijmissen and Horssen [23]. The difference between the two sets of results is very small and is well within 0.0036%. Secondly, the natural frequencies of a standing Timoshenko beam with clamped-free BCs. subjected to the gravity acceleration are listed in Table 3. The first ten dimensional frequencies ω (Hz) have been compared with Hijmissen and Horssen [23]. The excellent accuracy is detected and the differences between the results are very small and are within 0.0384%, then the proposed technique is very close to the exact solutions.

Table 2. The non-dimensional natural frequency λ^2 for uniform CF local beam

Case	I		II	
	r^2 = 0.01, s^2 = 2.8		r^2 = 0.001, s^2 = 0.5	
Mode number	Ref. [23]	Method	Ref. [23]	Method
1	3.2471	3.2471	3.5038	3.5038
2	14.803	14.8026	21.519	21.5191
3	32.415	32.4153	58.448	58.4478
4	49.649	49.6488	109.98	109.9815
5	65.263	65.2632	173.47	173.4722
6	70.555	70.5548	246.27	246.2743
7	84.075	84.0753	326.22	326.2190
8	92.021	92.0212	411.60	411.6015
9	105.87	105.8678	501.12	501.1166
10	113.75	113.7541	593.77	593.7673

Table 3. The effect of gravity on the natural frequencies ω (Hz) of uniform CF local beam

Mode number	The exact method [23]	The present Method	The error percent
	$r^2 = 6.30\times10^{-5}$, s^2 = 2.8, ε = 0.314		
1	0.2284	0.2283	0.0384
2	1.4513	1.4513	0.0028
3	4.0496	4.0496	0.0011
4	7.8792	7.8792	0.0002
5	12.903	12.9026	0.0034
6	19.055	19.0549	0.0004
7	26.265	26.2646	0.0017
8	34.455	34.4547	0.0009
9	43.549	43.5465	0.0058
10	53.467	53.4614	0.0104

Thirdly, the first five dimensionless natural frequencies of a Timoshenko beam are displayed for PP, CP, CC and CF boundary conditions are presented for various small scale effects α and L/d = 10, in Table 4. Where the other parameters of beam according to [13] are: diameter d = 0.678 nm, lengths L = 10d, and the following assumed mechanical parameters: Young's modulus E = 5.5 TPa, Poisson's ratio ν = 0.19, effective tube thickness t = 0.066 nm, shear correction factor K_s = 0.563. In Table 4, the frequencies have been compared by Wang et al. [13]. Note that the results associated with α = 0 correspond to the local TBT frequencies. The excellent accuracy and agreement are achieved between the results of the present method and the exact method [13] for local frequencies and also there is a rate of convergence for an adequate number of grid points. Although, for nonlocal frequencies, the result of the proposed technique is very close to the exact solution [13], but there is a critical difference between the present and exact procedures. Wang et al [13] used the constitutive relation to the shear stress and strain as the same as in the local beam theory, however, in the present method according to Ref. [4], the constitutive relation for the shear stress and strain

are considered as the nonlocal beam theory. Hence the present method is more complete and more accurate than Ref. [13].

Finally, the first four frequency parameters of the present method and those obtained by Farchaly and Shebl [33] and Chen [34] are shown in Table 5. The rotary inertia parameter $r^2=I/AL^2=0.01$ and shear deformation parameter $s^2=Er^2/Gk=0.03$ are considered, and also three values of compressive axial load parameter PL^2/EI, 0, 1 and 10, are considered. As it can be observed from the Table, the present results yield excellent agreement with those of [33,34]. The difference between the two sets of results is small and well within 0.0280%. As the compressive axial load is increased, natural frequencies of all modes are reduced.

6.2. The Numerical Examples

In this section, the bending vibration characteristics of the NUTNB will be examined. The effect of the varying cross-section area, small scale, shear deformation, rotational moment of inertia, acceleration gravity and the self-weight of the nano-beam on the non-dimensional natural frequencies and normalized mode shapes is demonstrated. The following parameters, material and geometric properties used in computing the numerical values are E = 30 MPa [12], ρ = 2300 kg/m^3, L = 10 nm, h = varied, ν = 0.3, K_s = 5/6 and g = 9.81 m/s^{-2}.

The problem can be solved for each arbitrary $A(x)$. In this paper, we assume the $A(x)$ as,

$$A(x)=1-\frac{x^2}{20\ell^2} \tag{47}$$

To study the effect of nonlocal parameter, frequency ratio is defined as,

$$\text{Frequency ratio}=\frac{\text{Frequency using nonlocal theory}}{\text{Frequency using local theory}} \tag{48}$$

6.2.1. The Convergence of N in GDQM

Minimum number of grid points is performed by the convergence test in GDQM [14] using the following equation required to obtain stable and accurate results. The error percent vs. number of grid points for the fundamental frequency (μ = 0.1) for a Pinned-Pinned beam is shown in Fig. 1. It can be noted form Fig. 1, that eleven number grid points are sufficient in resulting converged solution.

$$\text{Error percent}=\frac{100\times(\text{Present result-Converged result})}{\text{Converged result}} \tag{49}$$

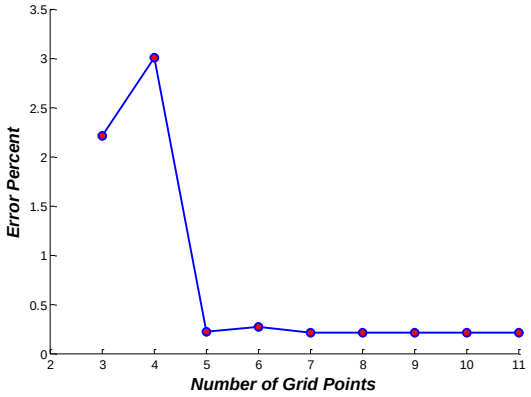

Figure 1. The convergence of nonlocal results by GDQM

Table 4. First five natural frequencies of uniform beam with L/d = 10

BCs.	Mode number	α									
		0		0.1		0.3		0.5		0.7	
		Present	Ref. [13]	Present	Ref. [13]	Present	Ref. [13]	Present	Ref. [13]	Present	Ref. [13]
Pinned Pinned	1	3.0929	3.0929	3.0210	3.0243	2.6385	2.6538	2.2665	2.2867	1.9899	2.0106
	2	5.9399	5.9399	5.4657	5.5304	4.0663	4.2058	3.2713	3.4037	2.7968	2.9159
	3	8.4444	8.4444	7.2037	7.4699	4.8761	5.2444	3.8474	4.1644	3.2690	3.5453
	4	10.6262	10.626	8.3851	8.9874	5.3806	6.0228	4.2128	4.7436	3.5713	4.0283
	5	12.5413	12.541	9.1905	10.206	5.7140	6.6333	4.4571	5.2009	3.7743	4.4107
Clamped Pinned	1	3.7845	3.7845	3.6846	3.6939	3.1711	3.2115	2.6966	2.7471	2.3553	2.4059
	2	6.4728	6.4728	5.9353	6.0348	4.3904	4.6013	3.5310	3.7312	3.0198	3.2003
	3	8.8212	8.1212	7.5104	7.8456	5.0816	5.5482	4.0139	4.4185	3.4127	3.7666
	4	10.8800	10.880	8.5826	9.2751	5.5161	6.2641	4.3241	4.9460	3.6677	4.5528
	5	12.7075	12.707	9.3194	10.433	5.8062	6.8277	4.5335	5.3640	3.8408	4.8326
Clamped Clamped	1	4.4491	4.4491	4.3269	4.3471	3.7032	3.7895	3.1357	3.2420	2.7327	2.8383
	2	6.9524	6.9524	6.3546	6.4952	4.6553	4.9428	3.7269	3.9940	3.1808	3.4192
	3	9.1626	9.1626	7.7884	8.1969	5.2714	5.8460	4.1729	4.6769	3.5522	3.9961
	4	11.1126	11.113	8.7619	9.5447	5.6290	6.4762	4.4105	5.1131	3.7399	4.3455
	5	12.8627	12.863	9.4384	10.649	5.8924	7.0170	4.6077	5.5283	3.9066	4.6986
Clamped Free	1	1.8610	1.8610	1.8467	1.8650	1.7514	1.8999	1.6223	2.0024	1.4986	-
	2	4.4733	4.4733	4.2956	4.3506	3.4516	3.6594	2.7448	2.8903	2.2849	-
	3	7.1072	7.1072	6.4181	6.6091	4.6091	5.0762	3.6883	-	3.1592	-
	4	9.3813	9.3813	7.8500	8.3151	5.1542	5.7875	3.9894	-	3.3525	-
	5	11.3811	11.381	8.8244	9.6705	5.5939	6.5843	4.3838	-	3.7244	-

6.2.2. Effect of Nonlocal Parameter

The non-dimensional local and nonlocal frequencies are computed by using the present GDQM for the NUTNB with L/h=100 and various values of small scale for six boundary conditions and the results are listed in Table 6. The effect of the nonlocal parameter α is to reduce the natural frequencies, as it can be seen from the results, which are presented in Table 6.

Hence, as the small scale coefficient increases, the frequencies obtained for the nonlocal beam become smaller the local counterpart, and so the frequency ratio is always smaller than unity. This reduction is especially significant for the higher vibration modes. Based on the results in Table 6, it is found that for constant nonlocal parameter α, among all of the boundary conditions, clamped-clamped contain largest frequency and pinned-slide contain smallest frequency. From Table 6, it is observed that fundamental frequency for clamped-free approximately remains unchanged with the increase in the nonlocal parameters. Table 6 implies that the frequencies for non-uniform (tapered) nano-beam are smaller than the same frequencies of uniform nano-beam. The above result can be demonstrated in Figs. 2 to 4.

To demonstrate the effect of higher modes, frequency ratio for various nonlocal parameters is plotted in Figs. 3 and 4, for non-uniform and uniform cross-section, respectively. From these figures, it can be obviously observed that as the nonlocal parameter value increases, the frequency ratio decreases. In addition, at higher mode numbers, all results converge to the local frequency at the higher lengths. This phenomenon is because of the increase in the interactions between atoms at small wavelengths at higher wave numbers [1].

Table 5. The comparison of first four dimensionless natural frequencies for a clamped–free uniform beam

Axial load	Method	r^2 = 0.01, s^2 = 0.03			
		Mode 1	Mode 2	Mode 3	Mode 4
p=0	Ref. [33]	1.799	3.820	5.642	6.967
	Ref. [34]	1.7964	3.8047	5.6170	6.9305
	Present	1.7985	3.8199	5.6423	6.9671
p=1	Ref. [33]	1.579	3.715	5.569	6.904
	Ref. [34]	1.5768	3.6982	5.5425	6.8666
	Present	1.5792	3.7145	5.5692	6.9043
p=10	Ref. [33]	2.199	4.720	6.171	-
	Ref. [34]	2.2009	4.7242	6.1811	-
	Present	2.1993	4.7197	6.1707	7.3434

6.2.3. The Effect of Gravity Acceleration

In Table 7, the non-dimensional first five frequency ratioes of a standing cantilever nano-beam are listed for uniform & non-uniform cross-section with $A(x)$ = 1- $0.05x^2$ and without & under gravity acceleration with gravity parameter ε = 0.9025 and L/h = 100.

As Table 7 shows quite clearly, in the case under gravity acceleration, the non-dimensional frequencies are less than the counterpart frequencies in the case without gravity acceleration. Hence the frequencies decrease due to the self-weighting for a standing cantilever beam. Based on the results in this Table, the fundamental frequencies at uniform cross-section are less than the same frequencies at a non-uniform cross-section for both cases under & without gravity (see Fig. 5).

It can be seen from Fig. 6 that the frequency ratio for uniform beam decreases more with increasing nonlocal parameters with respect to the non-uniform beam, and also the frequency ratio for uniform and non-uniform cross-section trends together with the increase of the mode number in standing cantilever nano-beam under gravity.

6.2.4. The Effect of Length

Figs. 7 and 8 show the variation of non-dimensional fundamental frequency ratio with the length of the beam for pinned-pinned and clamped-clamped boundary conditions with non-uniform cross-section $A(x)$ = 1- $0.05x^2$.

From Fig. 7(a), it can be comprehended that the space between the curves gradually decreases with the increase in the length of nano-beam. Further, for all curves, frequency ratio converges to one by increasing the length. It is apparent due to the fact that with the increase of length the effect of the nonlocal parameter decreases and therefore the frequency ratio tends to unity. As expected, this convergence is more rapid for the small values of nonlocal parameters. These results are similarly found from Fig. 7(b) for clamped-clamped boundary condition.

Fig. 8 shows the small-scale effect on the dimensionless fundamental natural frequency of NUTNB with lengths of L = 10, 15 and 20 nm [35]. As it is shown in Fig. 8, the small-scale effects decrease with an increase in the length of a nano-beam.

Table 6. First five non-dimensional frequencies of NUTNB with L/h = 100

BCs.	Mode number	α								
		0	0.01	0.02	0.03	0.04	0.05	0.06	0.07	0.08
Pinned Pinned	1	3.1300	3.1292	3.1267	3.1227	3.1171	3.1097	3.1010	3.0908	3.0793
	2	6.2556	6.2495	6.2312	6.2014	6.1608	6.1105	6.0517	5.9857	5.9138
	3	9.3787	9.3578	9.2970	9.2017	9.0736	8.9197	8.7498	8.5681	8.3800
	4	12.4976	12.4479	12.3071	12.0934	11.8168	11.5001	11.1677	10.8296	10.4956
	5	15.5993	15.5358	15.2626	14.9386	14.4850	13.8580	13.3321	12.8209	12.3355
Clamped Pinned	1	3.9164	3.9152	3.9117	3.9058	3.8976	3.8872	3.8747	3.8602	3.8438
	2	7.0372	7.0297	7.0074	6.9709	6.9215	6.8603	6.7892	6.7096	6.6233
	3	10.1577	10.1338	10.0659	9.9531	9.8074	9.6346	9.4426	9.2384	9.0278
	4	13.2729	13.2193	13.0652	12.8220	12.5187	12.1761	11.8141	11.4476	11.0871
	5	16.3769	16.2981	16.1023	15.5693	15.0497	14.4919	13.9305	13.3870	12.8727
Clamped Clamped	1	4.7003	4.6988	4.6943	4.6868	4.6765	4.6633	4.6475	4.6291	4.6083
	2	7.8072	7.7982	7.7717	7.7285	7.6699	7.5976	7.5136	7.4200	7.3186
	3	10.9286	10.9018	10.8232	10.6981	10.5345	10.3411	10.1269	9.8999	9.6668
	4	14.0427	13.9832	13.8119	13.5482	13.2174	12.8452	12.4535	12.0585	11.6714
	5	17.1634	17.0522	16.7389	16.2743	15.7188	15.1248	14.5292	13.9546	13.4127
Clamped Free	1	1.8883	1.8882	1.8882	1.8882	1.8882	1.8882	1.8882	1.8882	1.8882
	2	4.6907	4.6892	4.6846	4.6770	4.6663	4.6528	4.6365	4.6175	4.5959
	3	7.8269	7.8179	7.7913	7.7479	7.6892	7.6167	7.5325	7.4385	7.3370
	4	10.9434	10.9166	10.8380	10.7128	10.5491	10.3555	10.1411	9.9139	9.6805
	5	14.0593	13.9965	13.8387	13.5618	13.2189	12.8532	12.4620	12.0664	11.6784
Clamped Slide	1	2.3645	2.3643	2.3635	2.3623	2.3607	2.3586	2.3561	2.3530	2.3501
	2	5.4739	5.4705	5.4605	5.4439	5.4212	5.3926	5.3587	5.3199	5.2768
	3	8.5966	8.5823	8.5405	8.4731	8.3830	8.2739	8.1495	8.0139	7.8706
	4	11.7161	11.6783	11.5708	11.4025	11.1860	10.9350	10.6631	10.3810	10.097
	5	14.8176	14.7396	14.5473	14.2067	13.7950	13.3543	12.8958	12.4416	12.0178
Pinned Slide	1	1.5599	1.5598	1.5594	1.5586	1.5577	1.5565	1.5550	1.5533	1.5512
	2	4.6904	4.6878	4.6801	4.6674	4.6498	4.6278	4.6015	4.5714	4.5379
	3	7.8161	7.8040	7.7685	7.7111	7.6342	7.5407	7.4337	7.3165	7.1920
	4	10.9382	10.9047	10.8091	10.6588	10.4649	10.2392	9.9934	9.7373	9.4784
	5	14.0388	13.9847	13.7849	13.4851	13.1123	12.6974	12.2717	11.8478	11.4374

Table 7. First five non-dimensional frequency ratio of standing cantilever nano-beam under gravity acceleration with L/h = 100, ε = 0.9025

α		0		0.02		0.04		0.06		0.08	
Mode	Type	U	NU	U	NU	U	NU	U	NU	U	NU
1	NG	1.8750	1.8883	1.8744	1.8882	1.8727	1.8882	1.8698	1.8882	1.8658	1.8882
	G	1.8188	1.8320	1.8181	1.8318	1.8161	1.8313	1.8128	1.8304	1.8083	1.8291
2	NG	4.6928	4.6907	4.6847	4.6846	4.6608	4.6663	4.6219	4.6365	4.5697	4.5959
	G	4.6738	4.6716	4.6655	4.6653	4.6410	4.6464	4.6013	4.6156	4.5478	4.5736
3	NG	7.8496	7.8269	7.8108	7.7913	7.6999	7.6892	7.5302	7.5325	7.3194	7.3370
	G	7.8381	7.8153	7.7989	7.7792	7.6870	7.6760	7.5159	7.5175	7.3033	7.3196
4	NG	10.9821	10.9434	10.8718	10.8380	10.5703	10.5491	10.1452	10.1411	9.6656	9.6805
	G	10.9737	10.9345	10.8626	10.8287	10.5600	10.5386	10.1330	10.1288	9.6509	9.6656
5	NG	14.1096	14.0593	13.8866	13.8387	13.2507	13.2189	12.4743	12.4620	11.6939	11.6784
	G	14.0761	14.0240	13.8791	13.8174	13.2417	13.2198	12.4630	12.4516	11.6795	11.6644

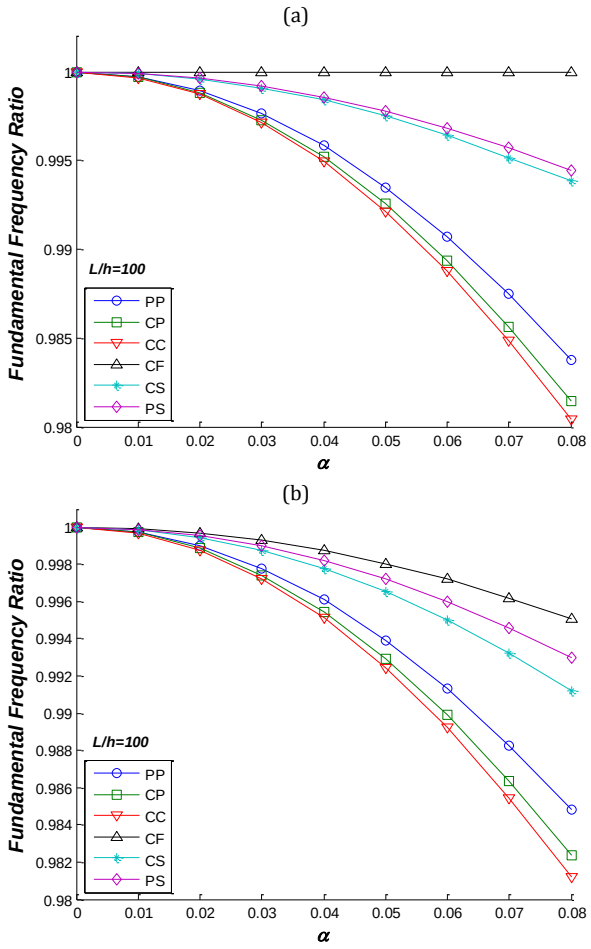

Figure 2. The variation of non-dimensional fundamental frequency ratio with the nonlocal parameter for various boundary conditions for (a) non-uniform nano-beam with $A(x) = 1- 0.05(x/l)^2$ and (b) uniform nano-beam

6.2.5. *The Effect of Axial Load*

Fig. 9 presents the influence of the tensional axial load on the pinned-pinned non-uniform nano beam with a variation of nonlocal parameters. The fundamental frequency ratio always decreases with the increase in nonlocal parameter; however, this decreasing of restraint will increases the tensional axial load. Further, when the axial load increases the nonlocal and local frequencies tend together, meanwhile, significantly increases the frequencies of NUTNB.

6.2.6. *The Normalized Mode Shapes*

Unlike for the pinned-pinned beam case where the mode shapes are not affected by the small scale effect parameter, the mode shapes of the clamped-clamped and clamped-pinned beam are significantly influenced by the small scale effect. The similar phenomenon is also found by Wang et al. [13] for linear vibration modes of the nonlocal Timoshenko beams and Yang et al. [36] for nonlinear vibration modes.

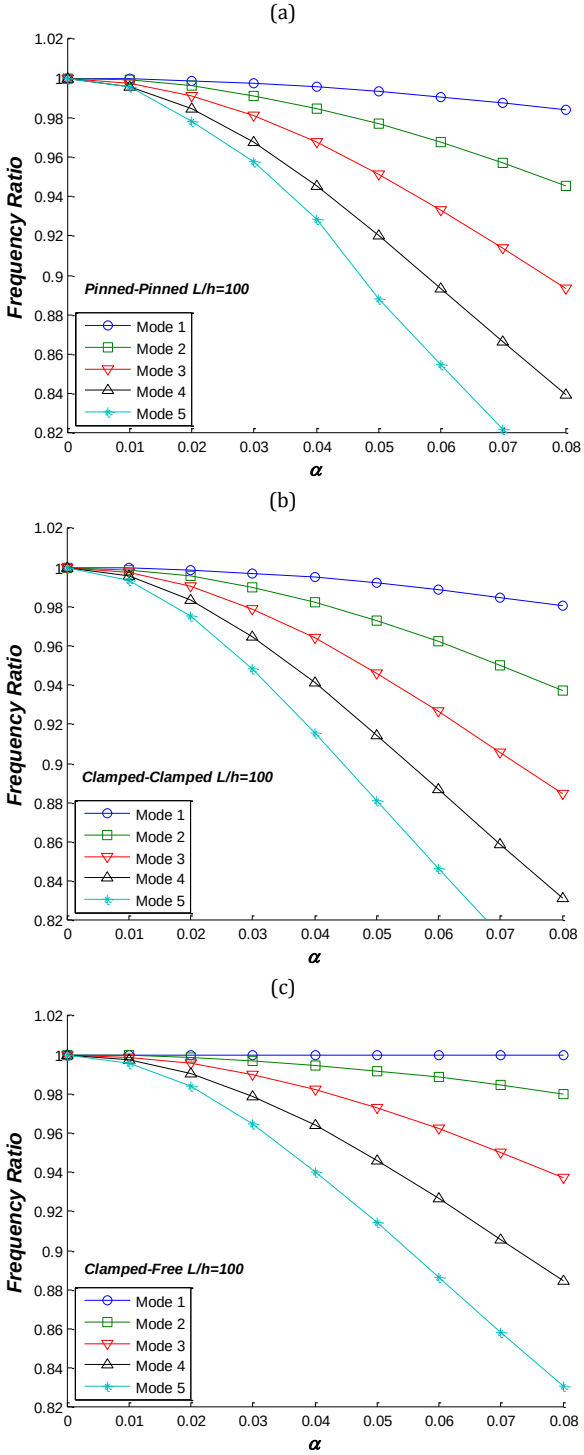

Figure 3. The variation of non-dimensional first five frequency ratio with the nonlocal parameter for NUTNB with $A(x) = 1-0.05(x/l)^2$ for (a) pinned-pinned, (b) clamped-clamped and (c) clamped-free

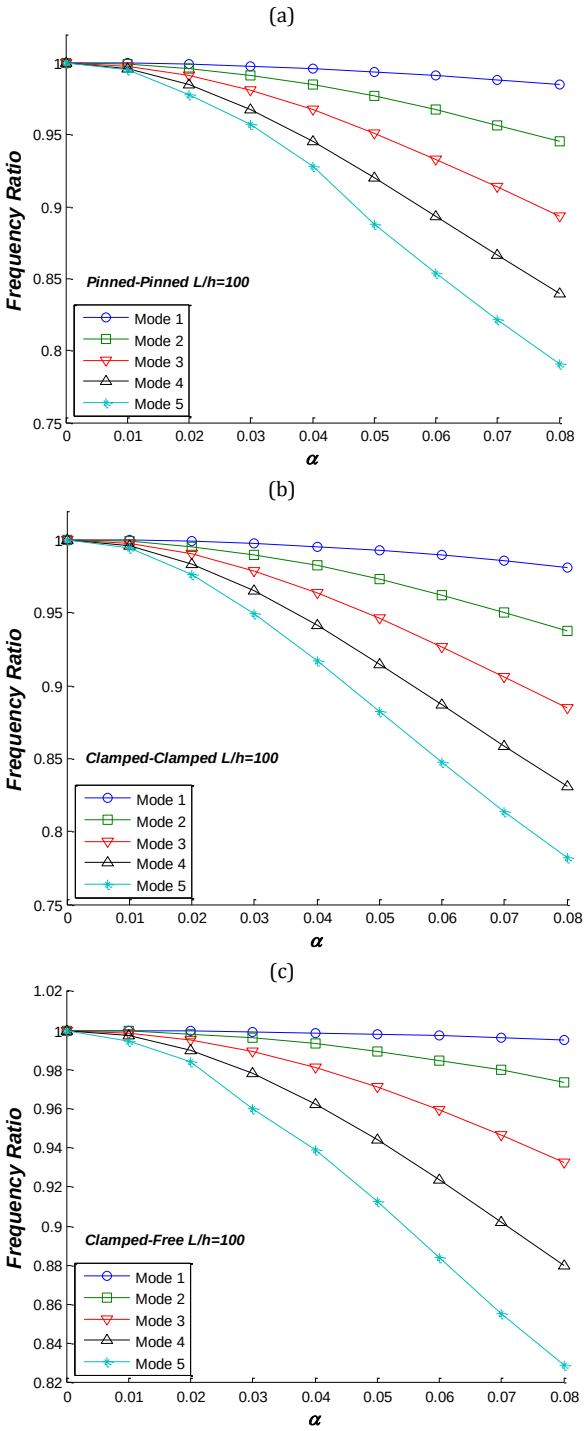

Figure 4. The variation of non-dimensional first five frequency ratio with the nonlocal parameter for uniform nano-beam for (a) pinned-pinned, (b) clamped-clamped and (c) clamped-free

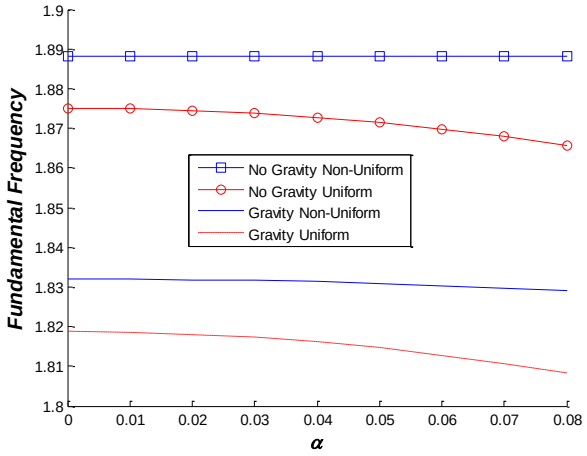

Figure 5. The variation of non-dimensional fundamental frequency with the nonlocal parameter for standing cantilever nano-beam without and under gravity acceleration and uniform and non-uniform

7. Conclusions

Transverse vibration characteristics have been investigated for a non-uniform Timoshenko nano-beam based on Eringen's nonlocal elasticity theory with axially loaded. A numerical approach (GDQM) has been used to study solving governing equations. Many typical results calculated by the presented method show excellent agreement with the exact results by other investigators. The same influence has been studied for the scale effect (nonlocal parameters), varying cross-section area, shear deformation, rotational moment of inertia, size of nano-beam, axial load, acceleration gravity and the self-weight of the NUTNB on the dimensionless natural frequencies. Based on the results, which have been discussed earlier, several conclusions can be addressed as follows:

(1) The small number grid points are sufficient in resulting converged solution and the presented work reflects the power of GDQM in solving non-uniform problems.

(2) The effect of the nonlocal parameter is to reduce the natural frequencies, hence the nonlocal frequencies are smaller than the local counterparts.

(3) The small scale effects are more significant for smaller size of nano-beam, larger nonlocal parameter and higher vibration modes.

(4) Among all of the boundary conditions (PP, CC, CP, CF, CS and PS), clamped-clamped (CC) contain largest frequency and pinned-slide (PS) contains smallest frequency.

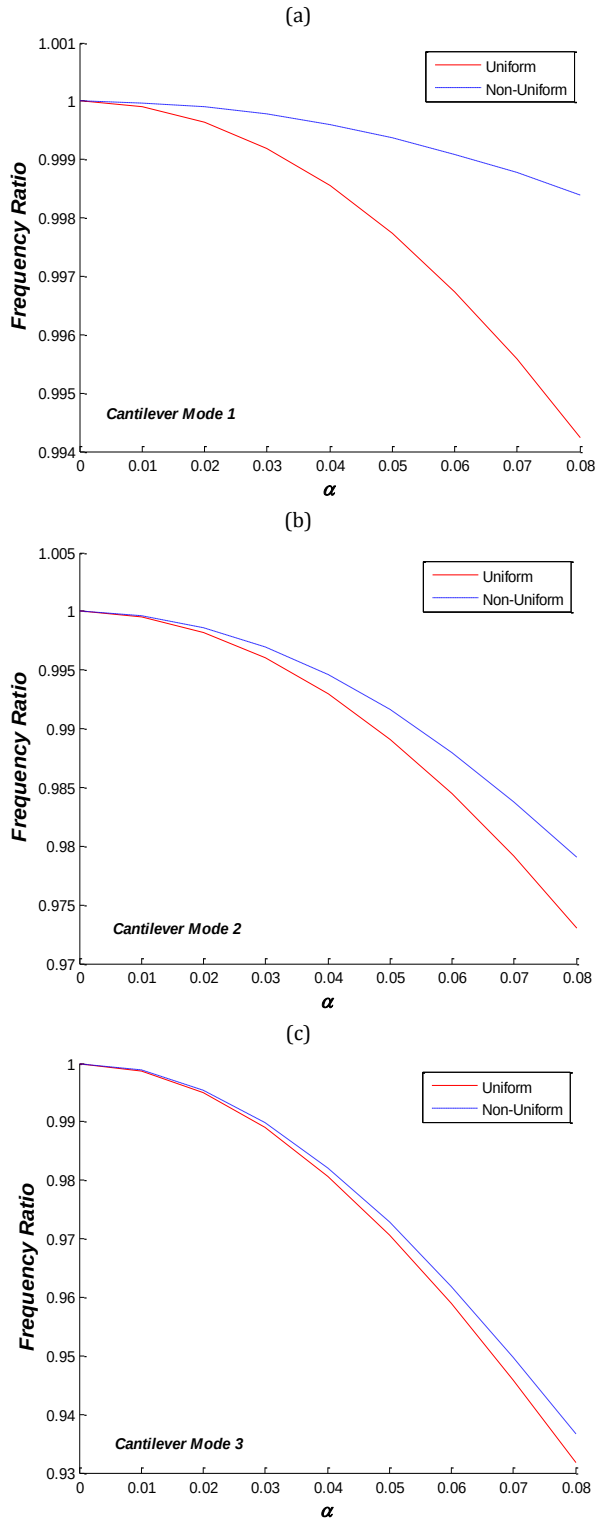

Figure 6. The variation of non-dimensional frequency ratio with the nonlocal parameter for standing cantilever nano-beam under gravity acceleration (a) mode 1, (b) mode 2 and (c) mode 3

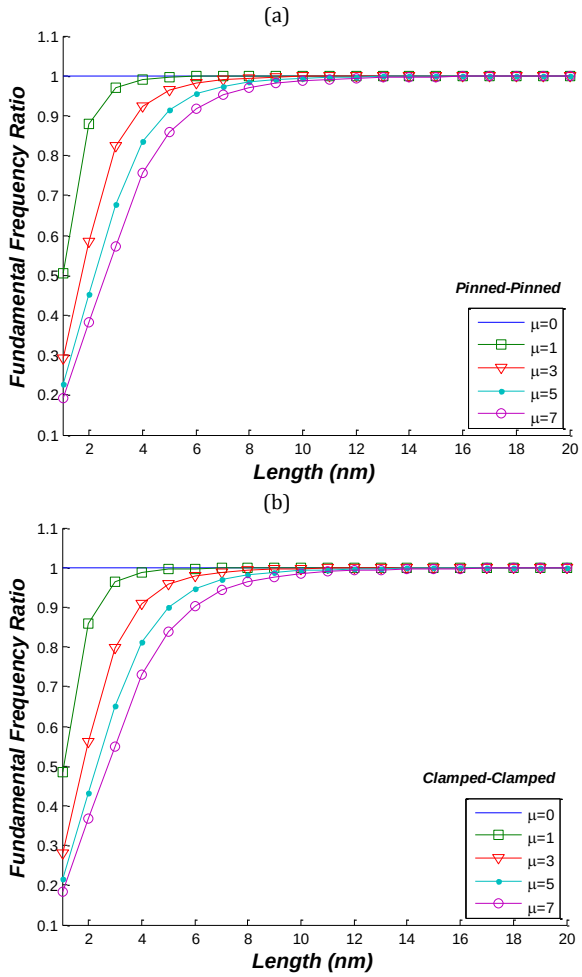

Figure 7. The variation of non-dimensional fundamental frequency with length of beam with various values of the nonlocal parameter for non-uniform cross-section (a) pinned-pinned and (b) clamped-clamped

(5) The frequency for non-uniform (tapered) nano-beam is smaller than the same frequencies of uniform nano-beam.

(6) Due to gravity acceleration and self-weighting (or distributed compressive axial force) for a standing cantilever beam, the non-dimensional frequencies are less than the counterpart frequencies in the case without gravity acceleration. While the increase in the tensional axial load always causes an increase in the frequencies of NUTNB.

(7) In general, the frequency ratio for uniform beam decreases more by increasing nonlocal parameters with respect to the non-uniform beam for all of the boundary conditions of nano-beam.

(8) The small scale effect parameter is more significant for the mode shapes of the clamped-clamped and clamped-pinned unlike the mode shapes for the pinned-pinned beam case.

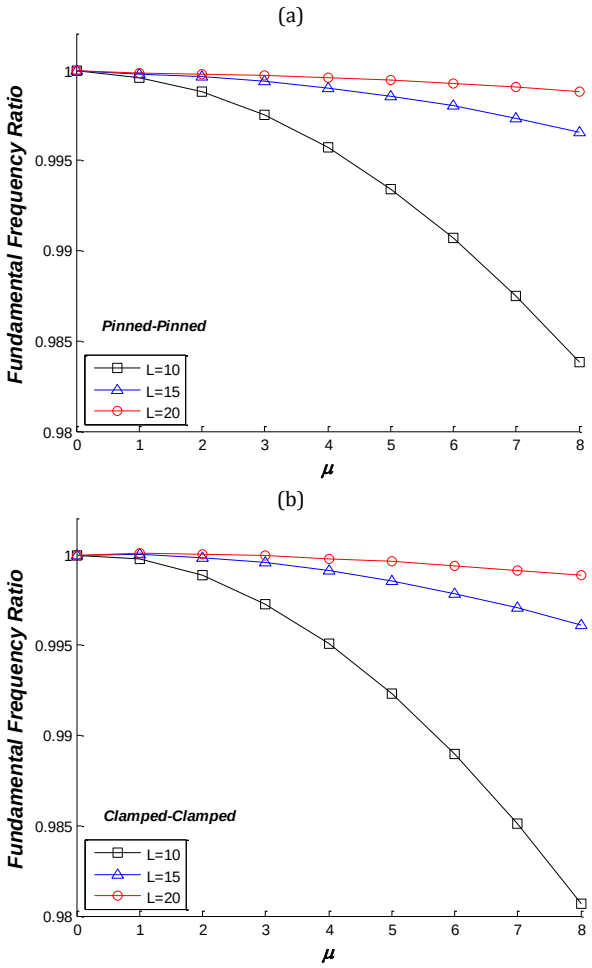

Figure 8. The variation of non-dimensional fundamental frequency with the nonlocal parameter for various values of length of beam for non-uniform cross-section, (a) pinned-pinned and (b) clamped-clamped

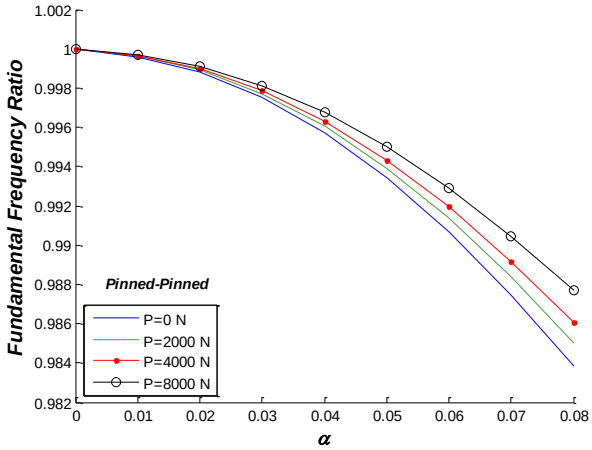

Figure 9. The influence of the tensional axial load on pinned-pinned non-uniform nano-beam with the variation of nonlocal parameters

Nomenclature

σ	nonlocal stress tensor
$t(x')$	classical, macroscopic stress tensor
K	kernel function
τ	material constant
e_0	constant appropriate to each material
a	internal characteristics length
l	external characteristics length
E	Young's modulus
G	shear modulus
γ	shear strain
μ	nonlocal parameter
M	nonlocal bending moment
Q	shear force
σ_{xx}	normal stress
σ_{xz}	transverse shear stress
A	cross-sectional area of the beam
K_s	shear correction factor of the TBT
ρ	mass density of the nano-beam
P	distributed axial load along x axis
W	amplitude of the generalized displacements
Φ	rotation of beam
ω	vibration frequency of NUTNB
λ	natural frequency
ζ	slenderness ratio
α	scaling effect parameter of the nano-beam
Ω	shear deformation parameter
$\bar{M}$	bending moment
$\bar{p}$	axial forces
V	shear forces
ε	gravity parameter
$\bar{p}_g$	coefficient of the axial force due to gravity
$\bar{P}_g$	function of the axial force due to gravity
x_j	nodes coefficients.
w_j	weighting coefficients.
C_{mij}	weighting coefficients for mth derivative
$w(x_j)$	function values at grid points

References

[1] Wang LF, Hu HY. Flexural Wave Propagation in Single-walled Carbon Nanotubes. *Phys Rev B* 2005; 71: 1–7.

[2] Eringen AC. Nonlocal Polar Elastic Continua. *Int J Eng Sci* 1972; 10: 1–16.

[3] Eringen AC, Edelen DGB. On Nonlocal Elasticity. *Int J Eng Sci* 1972; 10: 233–248.

[4] Eringen AC. On Differential Equations of Nonlocal Elasticity and Solutions of Screw Dislocation and Surface Waves. *J Appl Phys* 1983; 54: 4703–4710.

[5] Eringen AC. **Nonlocal Continuum Field Theories.** Springer-Verlag; 2002.
[6] Lu P, Lee HP, Lu C, Zhang PQ. Dynamic Properties of Flexural Beams using a Nonlocal Elasticity Model. *J Appl Phys* 2006; 99: 073510.
[7] Peddieson J, Buchanan GG, McNitt RP. Application of Nonlocal Continuum Models to Nanotechnology. *Int J Eng Sci* 2003; 41: 305–312.
[8] Reddy JN, Wang CM. Deflection Relationships between Classical and Third-order Plate Theories. *Acta Mech* 1998; 130(3–4): 199–208.
[9] Wang Q. Wave Propagation in Carbon Nanotubes via Nonlocal Continuum Mechanics. *J Appl Phys* 2005; 98: 124301.
[10] Wang Q, Varadan VK. Vibration of Carbon Nanotubes Studied using Nonlocal Continuum Mechanics. *Smart Mater Struct* 2006; 15: 659–666.
[11] Wang CM, Zhang YY, Ramesh SS, Kitipornchai S. Buckling Analysis of Micro- and Nano-rods/tubes based on Nonlocal Timoshenko Beam Theory. *J Phys D Appl Phys* 2006; 39: 3904–3909.
[12] Reddy JN. Nonlocal Theories for Bending, Buckling and Vibration of Beams. *Int J Eng Sci* 2007; 45: 288–307.
[13] Wang CM, Zhang YY, He XQ. Vibration of Nonlocal Timoshenko Beams. *Nanotechnology* 2007; 18: 1–9.
[14] Murmu T, Pradhan SC. Buckling Analysis of a Single-walled Carbon Nanotube Embedded in an Elastic Medium based on Nonlocal Elasticity and Timoshenko Beam Theory and using DQM. *Physica E* 2009; 41: 1232–1239.
[15] Şimşek M. Nonlocal Effects in The Forced Vibration of an Elastically Connected Double-carbon Nanotube System under a Moving Nanoparticle. *Comput Mater Sci* 2011; 50: 2112–2123.
[16] Lu P, Lee HP, Lu C, Zhang PQ. Application of Nonlocal Beam Models for Carbon Nanotubes. *Int J Solids Struct* 2007; 44: 5289–5300.
[17] Reddy JN. **Energy Principles and Variational Methods in Applied Mechanics.** John Wiley & Sons; 2002.
[18] Reddy JN. **Theory and Analysis of Elastic Plates and Shells.** Taylor & Francis; 2007.
[19] Reddy JN, Pang SD. Nonlocal Continuum Theories of Beams for The Analysis of Carbon Nanotubes. *J Appl Phys* 2008; 103: 023511.
[20] Hutchinson JR. Shear Coefficients for Timoshenko Beam Theory. *J Appl Mech* 2001; 68: 1–6.
[21] Meirovitch L. **Fundamentals of Vibrations.** McGraw-Hill; 2001.
[22] Ke LL, Xiang Y, Yang J, Kitipornchai S. Nonlinear Free Vibration of Embedded Double-walled Carbon Nanotubes based on Nonlocal Timoshenko Beam Theory. *Comp Mater Sci* 2009; 47: 409–417.
[23] Hijmissen JW, Horssen WTV. On Transverse Vibrations of a Vertical Timoshenko Beam. *J Sound Vib* 2008; 314: 161–179.
[24] Bellman R, Casti J. Differential Quadrature and Long-term Integration. *J Math Anal Appl* 1971; 34: 235–238.
[25] Bellman R, Kashef BG, Casti J. Differential Quadrature a Technique for The Rapid Solution of Nonlinear Partial Differential Equations. *J Comput Phys* 1972; 10: 40–52.
[26] Zong Z, Zhang Y. **Advanced Differential Quadrature Methods.** Chapman & Hall/CRC; 2009.
[27] Shu C. **Differential Quadrature and Its Application in Engineering.** Sprimger; 2000.
[28] Mestrovic M. Generalized Differential Quadrature Method for Timoshenko Beam. *MIT Conf Comput Fluid Solid Mech* 2003.
[29] Du H, Lim MK, Lin NR. Application of Generalized Differential Quadrature Method to Structural Problems. *J Num Meth Engrg* 1994; 37: 1881–1896.
[30] Du H, Lim MK, Lin NR. Application of Generalized Differential Quadrature to Vibration Analysis. *J Sound Vib* 1995; 181: 279–293.
[31] Mahmoud AA, Esmaeel RA, Nassar MM. Application of The Generalized Differential Quadrature Method to The Free Vibrations of Delaminated Beam Plates. *J Eng Mech* 2007; 14: 431–441.
[32] Wu T Y, Liu GR. A Differential Quadrature as a Numerical Method to Solve Differential Equations. *Comput Mech* 1999; 24: 197–205.
[33] Farchaly SH, Shebl MG. Exact Frequency and Mode Shape Formulae for Studying Vibration and Stability of Timoshenko Beam System. *J Sound Vib* 1995; 180: 205–227.
[34] Chen WR. Bending Vibration of Axially Loaded Timoshenko Beams with Locally Distributed Kelvin-Voigt Damping. *J Sound Vib* 2011; 330: 3040–3056.
[35] Arash B, Wang Q. A Review on The Application of Nonlocal Elastic Models in Modeling of Carbon Nanotubes and Graphenes. *Comput Mater Sci* 2012; 51: 303–313.

[36] Yang J, Ke LL, Kitipornchai S. Nonlinear Free Vibration of Single-walled Carbon Nanotubes using Nonlocal Timoshenko Beam Theory. *Physica E* 2010; 42: 1727–1735.